Bioorganic Chemistry 90 (2019) 103034

Contents lists available at ScienceDirect

Bioorganic Chemistry

journal homepage: www.elsevier.com/locate/bioorg

Ultrasound-assisted synthesis of novel chalcone, heterochalcone and bis-chalcone derivatives and the evaluation of their antioxidant properties and as acetylcholinesterase inhibitors

Efraín Polo[a], Nicol Ibarra-Arellano[a], Luis Prent-Peñaloza[a], Alejandro Morales-Bayuelo[b], José Henao[c], Antonio Galdámez[d], Margarita Gutiérrez[a,*]

[a] Laboratorio de Síntesis Orgánica, Instituto de Química de Recursos Naturales, Universidad de Talca, Casilla 747, Talca 3460000, Chile
[b] Ciencias de la Salud, Grupo de Investigaciones Básicas y Clínicas de la Universidad del Sinú (GIBACUS), escuela de medicina, Universidad del Sinú, seccional Cartagena, Colombia
[c] Grupo de Investigación en Química Estructural (GIQUE), Escuela de Química, Facultad de Ciencias, Universidad Industrial de Santander, A.A. 678, Carrera 27, Calle 9 Ciudadela Universitaria, Bucaramanga, Colombia
[d] Departamento de Química, Facultad de Ciencias, Universidad de Chile, Santiago 7800003, Chile

ARTICLE INFO

Keywords:
Chalcones
Bis-chalcones
Alzheimer's disease
Antioxidant
Molecular modeling

ABSTRACT

The chalcone and bis-chalcone derivatives have been synthesized under sonication conditions via Claisen-Schmidt condensation with KOH in ethanol at room temperature (20–89%). The structures were established on the basis of NMR, IR, Single-crystal XRD, and MS. The best compound **3u** had inhibitory activity ($\mathbf{IC_{50}}$ = **7.50 μM**). The synthesis, the antioxidative properties, chemical reactivity descriptors supported in Density Functional Theory (DFT), acetylcholinesterase (AChE) inhibition and their potential binding modes, and affinity were predicted by molecular docking of a number of morpholine-chalcones and quinoline-chalcone. A series of bis-chalcones are also reported. Molecular docking and an enzyme kinetic study on compound **3u** suggested that it simultaneously binds to the catalytic active site (CAS) and peripheral anionic site (PAS) of AChE. Moreover, the pharmacokinetic profile of these compounds was investigated using a computational method.

1. Introduction

Alzheimer's disease (AD) is the major cause of dementia (1 in 8 of people over 65 has AD in the USA). One hallmark of AD is the presence of senile plaques (PS) and neurofibrillary tangles (NFTs), which are formed due to the accumulation of β-amyloid peptide (Aβ) and hyperphosphorylated tau protein (p-tau), respectively. There is also a reduction in the number of neurons and synapses with marked cholinergic deficits [1]. Pharmacological treatment for AD mainly involves the use of cholinesterase inhibitors (galantamine, donepezil and rivastigmine) in the mild to moderate phases, and glutamatergic antagonists of the *N*-methyl-D-aspartate receptor (NMDAR) (memantine) in the moderate to severe phases of the disease. The use of anticholinesterases, although not preventing the progression of the disease, generates an improvement in the clinical manifestations of patients with AD, especially in the cognitive sphere [2,3].

Chalcones, bis-chalcones and their derivatives are attracting increasing attention due to numerous pharmacological applications [4]. Chalcones are the main precursors for the biosynthesis of flavonoids and isoflavonoids and exhibit various biological activities such as anti-tuberculosis agents [5], antiviral, anti-Inflammatory [6], antiplatelet [7,8], antimalarial [9,10], Tubulin inhibitors [11], Anti-Leishmanial agents [12], and others [4].

On the other hand, quinolinyl chalcones have showed a wide range of biological activities such as Antibacterial [13], antimalarial [14], anti-inflammatory [15], anti-infective [16], DNA gyrase inhibitor [17], antitumor [18], antimycotic [19], reverse-transcriptase inhibitor [20], and antiulcer [21].

A variety of methods are available for the synthesis of chalcones (Fig. 1) [22]. Traditionally, chalcones could be obtained via Claisen–Schmidt condensation carried out in basic or acidic media under homogeneous conditions [23]. The heterogeneous catalysts also have been used for Claisen–Schmidt condensation, including Lewis acids, Brønsted acids, solid acids, and solid bases with moderate success

* Corresponding author.
E-mail address: mgutierrez@utalca.cl (M. Gutiérrez).

https://doi.org/10.1016/j.bioorg.2019.103034
Received 26 February 2019; Received in revised form 17 May 2019; Accepted 3 June 2019
Available online 08 June 2019

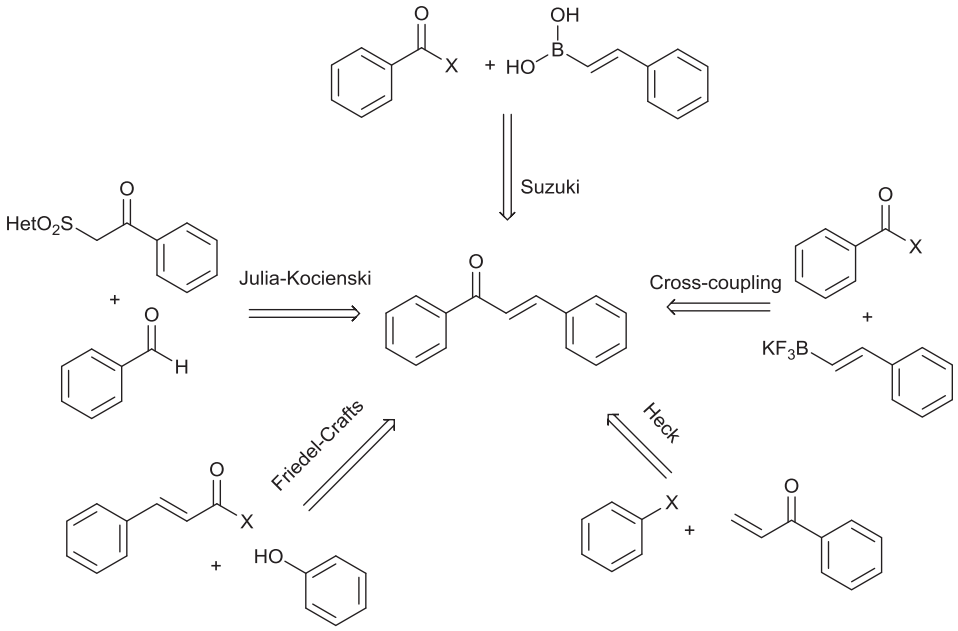

Fig. 1. Non-conventional synthesis of chalcones.

[24–29]. Several research works have demonstrated that many organic reactions have been accelerated by ultrasonic irradiation, for example, polymer synthesis, electron transfer reaction, cycloaddition reactions, phase transfer reactions, and others [30]. Most of them depend on the presence of specific catalysts. The reaction of Claisen-Schmidt to obtain chalcones has also been previously reported through the use of specific catalysts, KF-Al_2O_3, the telluroxide (bis(*p*-methoxyphenyl)), and 2-2-bipyridine complex of $Co(OAc)_2$ were used as basic catalysts [31].

2. Results and discussion

2.1. Chemistry

We have synthetized a library of seventeen chalcones and seven symmetric bis-chalcones with moderate to good yield (Table 1) using simple starting material and ultrasound (US) as a source of energy. US is well known for better yields, short reaction time, and for its clean process [32]. Hence, US methodology is considered an ecofriendly methodology. It is worth mentioning here that reaction time was reduced considerably with respect to the conventional methodology. That methodology has a reported reaction time between 3 and 72 h [33,34]. In this work, all the compounds were prepared in a maximum time of 20 min. To prepare compounds **3a–l** and **3m–s**, the aldehyde and bis-aldehyde components were kept, respectively, and different aromatic ketones with electron-withdrawing groups (EWG) and electron-releasing groups (ERG) were used. The results obtained show that there isn't a specific trend when the substituents are EWG or ERG. However, there is an improvement in the yield when the number of substituents increases, for example, compounds **3b**, **3i,** and **3j**. In the same way, there is an improvement in the yield when the electronegativity of halogen decreases (compounds **3d**, **3h,** and **3k**). Table 1 show structures of compounds synthetized, activities, and yield. Compounds **3d**, **3e**, **3h**, **3k,** and **3l**, were previously reported as intermediate for the synthesis of dihydropyrazole [35,36]. On the other hand, **3n–s** bis-chalcones were prepared to obtain different heterocycles [37,38,47,48,39–46].

The structure of **3a** and **3e** were further confirmed by the Single-crystal X-ray diffraction technique. The skeleton of these molecules is depicted in Table 1 and a summary of crystallographic data is given in Table 1S (supplementary materials). The torsion angle of C14-C13-C12-C11 are 166.6(2)° and −177.0(4)° in **3a** and **3e**, respectively. The Cremer and Pople puckering parameters of 6-membered ring (O1/C1-C4/N1) in **3a** are Q1 = 0.414(3) Å, θ = 6.1 (4)° and φ = 30.0 (5)° [49]. The six-membered ring adopts a half-chair conformation. The torsion angle of C17-O3-C20-C18 is −15.82(5)° in **3a**, N1-*C*2 bonds ranging from 1.413 to 1.416 Å in **3a** and **3e.** All relevant structural parameters (bond distances and angles) are as expected and in acceptable agreement with other organic molecules [50]. Moreover, in the crystal packing of **3a**, the molecules are linked *via* C-H···π interactions. The C3-H3B···*Cg1* [symmetry code: -x,1-y,2-z] and C21-H21···*Cg2* [symmetry code: 1-x,1-y,2-z] distances are 2.97 and 2.92 Å. Crystal packing of **3e** show a C19-H19···O2 intermolecular contact with a H···O bond distance of 2.60 Å [An angle of 135.00°]. Crystallographic data reported in this paper for **3a** and **3e** compounds have been deposited at the Cambridge Crystallographic Data Center (CCDC), No. 1867175 and 1867174, respectively. Copies of the data can be obtained, free of charge, on application to CCDC 12 Union Road, Cambridge CB2 1EZ, UK (Fax: +44-1223-336033 or e-mail: deposit@ccdc.cam.ac.uk).

The ^{1}H NMR coupling constant analyses indicated that all hydrogen atoms of the olefinic carbon–carbon bond were in a *trans* configuration (*J* approximately 15 Hz). The existence of a carbonyl group conjugated with the olefinic carbon–carbon bond was confirmed from the infrared spectra as the carbonyl peak was observed at a lower wavenumber than a normal carbonyl peak (around 1650–1600 cm^{-1}). The existence of methoxy groups in **3b**, **3i,** and **3j** was confirmed by the chemical shifts near 3.9 ppm in the ^{1}H NMR spectra. The signal which appeared as a doublet near 7.00 could be attributed to olefinic protons. In addition, the signal which appeared in the region at d 7.6–8.7 as multiplets was due to the aromatic protons present in the molecules. It was further supported by the molecular ion showed in GC–MS corresponding to the molecular mass of compounds. Similarly, all other chalcones were characterized and the data are given in the experimental section.

2.2. Biological evaluation

All compounds synthesized were evaluated *in vitro* as dual acetylcholinesterase (AChE)-butyrylcholinesterase (BuChE) inhibitors according to the modified Ellman's method [51]. Galantamine, a well-known AChE inhibitor, was used as the positive control. The concentration of the compound required for 50% enzyme inhibition (IC_{50}) was calculated by means of regression analysis. All tabulated results in

Table 1
Chalcones, hetero-chalcones, and bis-chalcones synthetized.

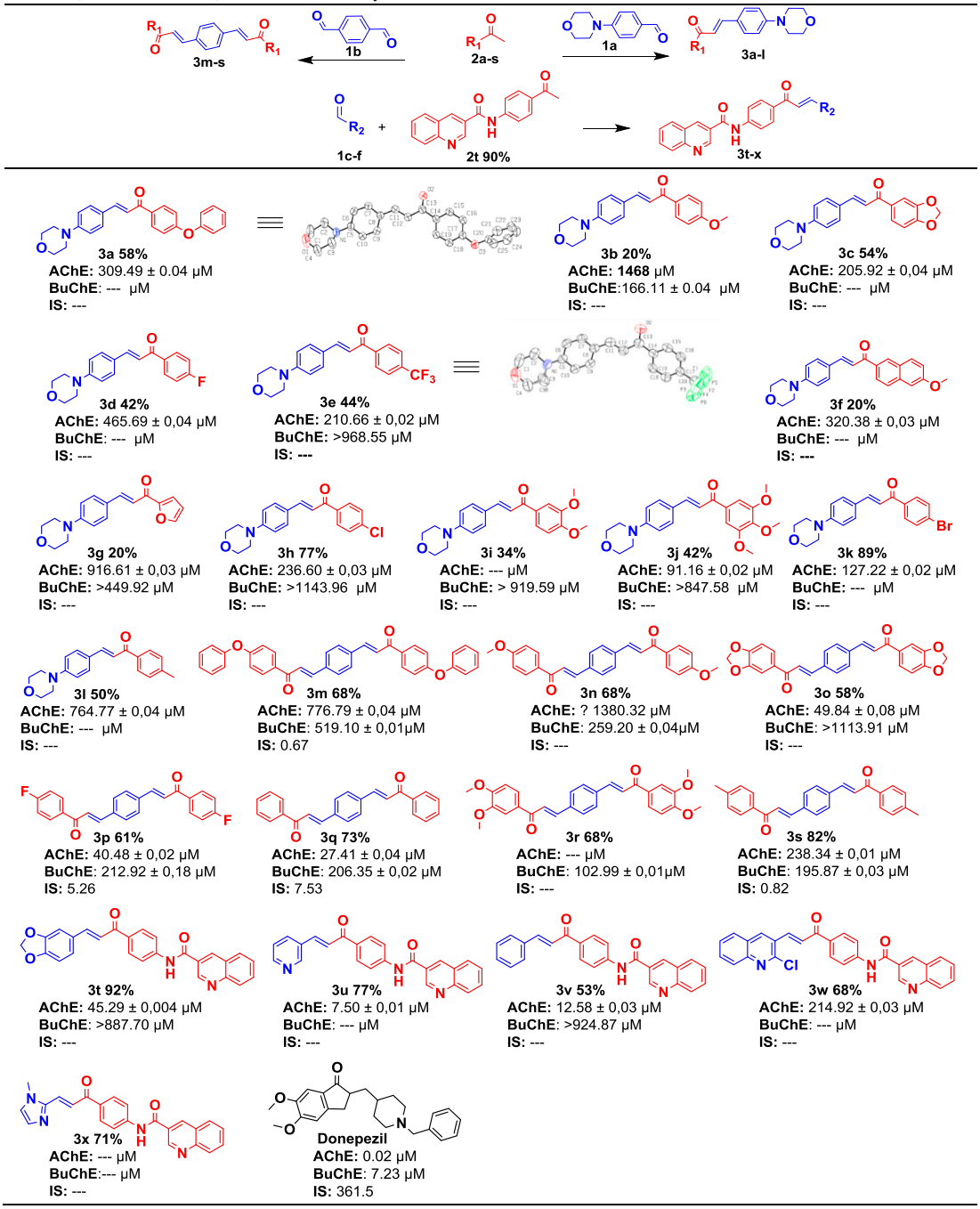

Table 2 are expressed in μM as means ± SEM, and were compared by using ANOVA analysis. A p value of less than 0.05 was considered significant. Details for pharmacological experiments are described in Materials and Methods as well as in previous works [52,53]. The inhibit ratio against AChE was calculated according to the absorbance of the product in the AChE-catalyzed reaction and the results are shown in Table 2.

The preliminary investigation demonstrated that morpholine chalcones **3a–l** showed poor inhibiting effect against AChE (IC_{50} > 50 μM). Bis-chalcone derivatives **3m–s** were found to present significant values in the range (27–1380 μM) where compound **3q,** containing moiety phenyl, showed the best inhibition (27.41 ± 0.038 μM). Electron donating groups (OCH_3 and CH_3) were present on the phenyl ring of the chalcone, which are associated with the decrease in activity. The quinoline based chalcones exhibited better inhibition values. Among them, compound **3u** contained the 3-pyridin group; it was found to have the most potent inhibitory activity with IC_{50} value 7.50 ± 0.011 μM. Compounds **3o–q**, **3t**, and **3v** have also considerable inhibitory values since their IC_{50} values were lower than 50 μM.

Based on the obtained results in the cholinesterase inhibition, and with the aim of assessing the kinetic mode of AChE inhibition of the target compounds, the most active compound **3u** was subjected to a kinetic study. For this purpose, the rate of enzyme activity was measured at eight different concentrations of substrate Acetylthiocholine iodide (ATC). The obtained Michaelis–Menten parameters along with the Lineweaver–Burk plots (Fig. 2) allowed us to conclude that

Table 2
Acetyl- and butyryl-cholinesterase inhibitory activities of compounds (**3a–w**).

Compound	Anticholinesterase assay		Compound	Anticholinesterase assay	
	AChE (μM)[a]	**BuChE (μM)**[a]		**AChE (μM)**[a]	**BuChE (μM)**[a]
3a	309.49 ± 0.04	–	**3m**	776.79 ± 0.04	519.10 ± 0.01
3b	> 1468	166.11 ± 0.04	**3n**	> 1380,32	259.20 ± 0.04
3c	205.92 ± 0,04	–	**3o**	49.84 ± 0.08	> 1113,91
3d	465.69 ± 0,03	–	**3p**	40.48 ± 0.02	212.92 ± 0.18
3e	210,66 ± 0,02	> 968.55	**3q**	27.41 ± 0.04	206.35 ± 0.02
3f	320.38 ± 0,03	–	**3r**	–	102.99 ± 0.01
3g	916.61 ± 0,03	> 449.9	**3s**	238.34 ± 0.01	195.87 ± 0.03
3h	236,60 ± 0,03	> 1143,96	**3t**	45,29 ± 0,004	> 887,70
3i	–	> 919.59	**3u**	7.50 ± 0.01	–
3j	91,16 ± 0,02	> 847.58	**3v**	12,58 ± 0,03	> 924,87
3k	127.2 ± 0,02	–	**3w**	214.92 ± 0,03	–
3l	764.77 ± 0,07	–	**Galantamine** [a]	0.57 ± 0,5	8.08 ± 0,02

[a] IC_{50} ± SEM.

Table 3
Antioxidant activity results for the most active compounds, DPPH and ABTS assays.

Compound	Antioxidant assay	
	DPPH assay IC_{50} (μg/mL)[a]	**$ABTS^+$ assay IC_{50} (μg/mL)**[a]
3e	≥100	199.60 ± 3.7
3m	≥100	173.59 ± 2.0
3o	99.03 ± 3.8	219.66 ± 1.5
3p	131.33 ± 2.7	254.49 ± 3.8
3s	185.97 ± 2.4	115.35 ± 3.3
Ascorbic acid[b]	1.5 ± 0.2	27.62 ± 3.5

[a] Values expressed are mean ± SEM of three parallel measurements ($p < 0.05$).
[b] Reference compound.

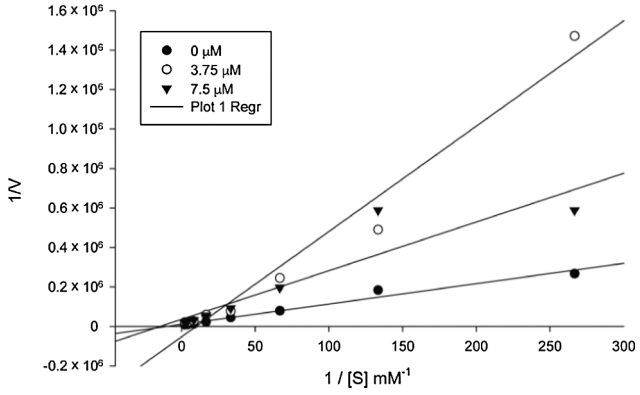

Fig. 2. The Lineweaver–Burk plot of AChE (0.02 U) with an Acetylthiocholine substrate in the absence and presence of inhibitor **3u**.

compound **3u** would display a mixed-type inhibition against AChE with variation in Km and Vmax values. The compound **3u** showed Km values of 9.71×10^{-4}, 1.89×10^{-4}, and 4.05×10^{-4} μM and Vmax of 9.6×10^{-5}, 1.89×10^{-5}, and 2.79×10^{-5} mol/min, respectively.

2.3. Theorical studies

Molecular docking of the most active compounds (**3q**, **3p**, **3u**, **and 3v**) was performed to explain the *in vitro* activity. The active-site of AChE is a cylinder cavity; Kryger et al. [54] have called this cavity a gorge. In the bottom of this gorge, compounds show a π-π interaction between the aromatic ring of Trp84 and one of the aromatic rings at the ends. That interaction is similar to the interaction showed by the benzyl group from donepezil (see Fig. 3).

In the middle of the gorge, a π-π interaction is observed between Phe330 and the aromatic ring located in the center of each structure. The interaction of the aromatic moiety of Phe330 is important because this connects the peripheral site and anionic subsite in the active site. That is to say, both the orientation and interaction of the aromatic ring of Phe330 influences the entry of compounds at the bottom of the gorge. In the entrance of the gorge, a π-π interaction is perceived between the aromatic ring from the other end of the molecule and the aromatic ring of Trp279. This interaction is presented between indanone moiety of donepezil and Trp279, too. This peripheral interaction is relevant due to the hydrophobic environment; i.e. it can serve as a filter to allow which molecule can enter the cavity [54].

Lipophilicity is a significant physicochemical property determining distribution, bioavailability, metabolic activity, and elimination. Apart from the important role of lipophilicity for the kinetics of biologically active compounds, antioxidants of hydrophilic or lipophilic character are both needed to act as radical scavengers in the aqueous phase or as chain-breaking antioxidants in biological membranes. A perusal of log P and IC_{50} values in Tables 1, 2, and 4 revealed that the role of lipophilicity on the inhibition of AChE wasn't well defined in this series of compounds. Analysing this data set, lipophilicity did not seem to affect absolutely the AChE inhibition in compounds **3a–s**. Within the chalcone morpholine subgroup compound, the **3 g** lower log P value (2.920) was correlated to higher activity (916.61 ± 0.033 μM). This concept was not followed by the bis-chalcones group, compound **3q** showed log P (5.372) and IC_{50} (27.41 ± 0.038 μM). The same trend was present for quinoline-chalcones where log P minimum was 3.772, associated to lower activity (7.50 ± 0.011 μM).

Chalcones derivatives have showed high capacity for the scavenging of free radicals' generation [55]. Chu et al. synthetized a set of amidochalcones developed by the Claisen-Schmidt methodology and tested their antioxidant activity in different *in vitro* systems like hydrogen peroxide scavenging activity, DPPH radical scavenging activity, ferrous reducing power, and nitric oxide radical scavenging activity. Their results show these compounds as potential antioxidant agents with good activity compared with the ascorbic acid used as Ref. [56]. Taking into account the previously described, we have used two different types of assays to measure *in vitro* antioxidant activity: (a) the interaction with the stable free radical DPPH and (b) the interaction with the water-soluble azo compound $ABTS^+$ where ascorbic acid was used as a positive control. The effect of the fluorine atom can be analyzed by comparing compound **3e** and compound **3p**. In **3e**, the F contained a compound at the 4th position of the phenyl ring, having better activity than CF_3 group in the 4th position of **3p**. In the DPPH assay, the IC_{50} values of the compounds (**3a–m**) were lower than 100 μg/mL. Compound **3o** exhibited better DPPH free radical scavenging activity with (IC_{50}: 99.03 ± 3.8 μg/mL). In the ABTS assay, among the tested compounds, **3m** and **3s** showed the best ABTS cation radical scavenging

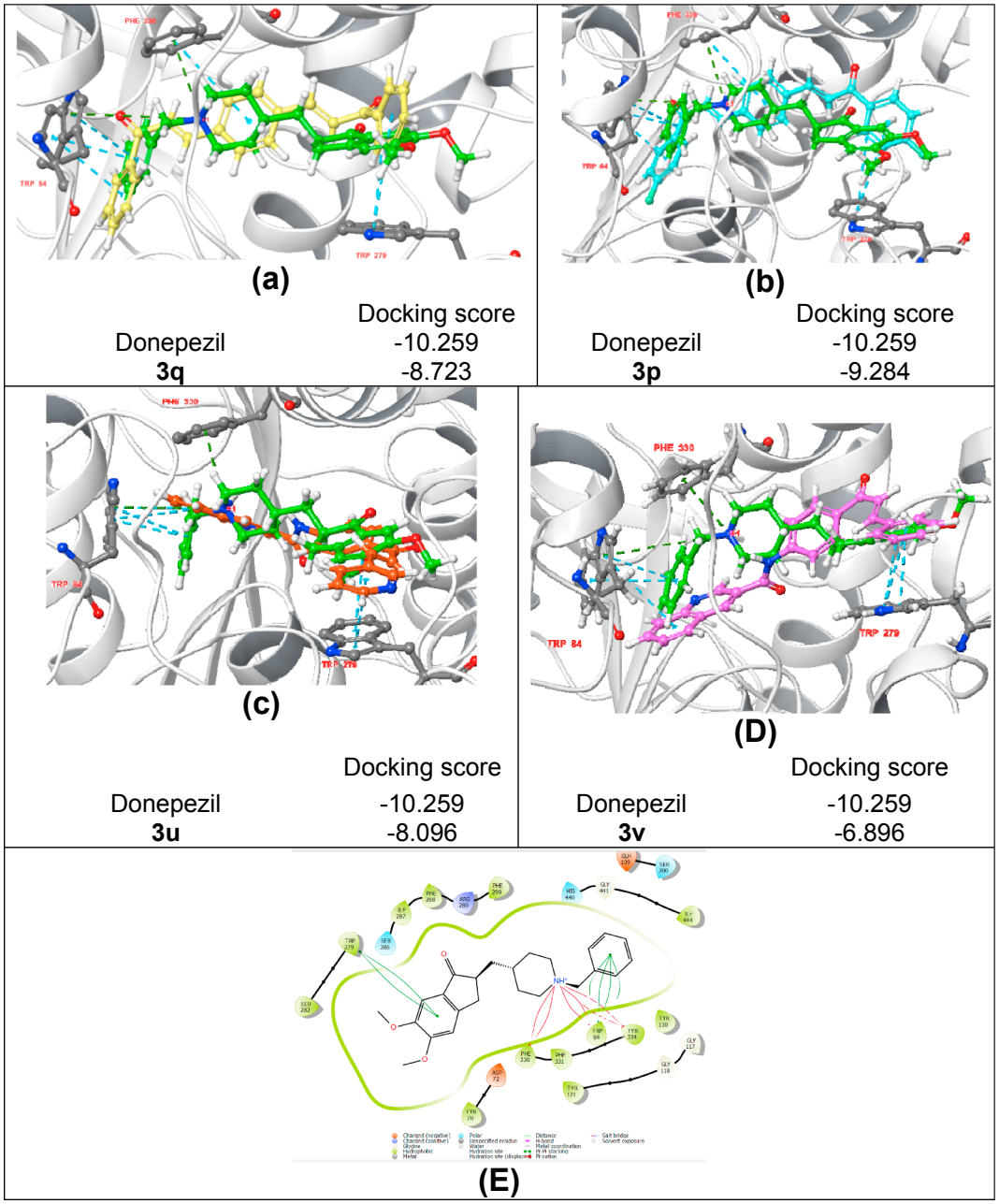

Fig. 3. Molecular docking between the most active compounds against AChE binding site. Docking pose of compound **3q** (a), **3p** (b), **3u** (c) and **3v** (D). Compound reference (donepezil) is represented in green. Protein backbone and principal residues of interaction are in cartoon and sticker presentation. (E) 2D representation of principal interaction of donepezil in AChE active-site.

activity with IC_{50} values of 173.59 ± 2.0 and 115.35 ± 3.3, respectively. With the exception of compounds **3n–p**, this series showed IC_{50} values that were higher than 200 μg/mL (Table 3).

In Figs. 4 and 5, the Fukui functions $\langle f_k^+ \rangle \approx |LUMO|^2$ and $\langle f_k^- \rangle \approx |HOMO|^2$ are shown for the most active compound **3u**. The Fukui functions in Figs. 4 and 5 represent the zones where it is possible to carry out stabilization by the retro-donor process on the active site for the compound with the best activity. These contours are very similar in both functions and also can be related with the stabilization through a retro-donor process.

The main zone for the stabilization with the highest surfaces is the carbonyl groups (H-bond acceptor) and the amino groups (H-bond donor).

In Table 4, the global reactivity indices for the compounds analyzed are shown. The compounds with higher biological activity are **3q**, **3u**, and **3v** (see Table 4). They have chemical potential: **3q** ($\mu = -4.2153$ eV), **3u** ($\mu = -4.4741$ eV), and **3v** ($\mu = -4.0028$ eV); chemical hardness: **3q** ($\eta = 3.4112$ eV), **3u** ($\eta = 3.9516$ eV), and **3v** ($\eta = 4{,}0028$ eV); chemical softness: **3q** ($S = 0{,}2931\ eV^{-1}$), **3u** ($S = 0{,}2530\ eV^{-1}$) and **3v** ($S = 0{,}2498\ eV^{-1}$); and electrophilicity: **3q** ($\omega = 2.6045$ eV), **3u** ($\omega = 2.5328$ eV), and **3v** ($\omega = 2.3175$ eV). From these results, we can see the reactivity properties to understand the non-covalent activity in a quantitative form. Additionally, the electrophilicity values in particular suggest stabilization through a retro-donor process.

The compounds with the higher electrophilicity values are **3m** and **3x**. These reactivity parameters show the stabilization of the electron cloud when it is saturated by electrons from the external environment. These values obtained give an idea about the stabilization process on the active site through non-covalent interactions due to the presence of

Table 4
Global reactivity descriptors.

Compound	C. Potential (eV)	C. Hardness (eV)	Softness $(eV)^{-1}$	Electrophilicity (eV)
3a	−3.4900	3.5982	0.2791	1.6925
3b	−3.4482	3.6284	0.2756	1.6385
3c	−3.4852	3.6050	0.2773	1.6847
3d	−3.5999	3.5595	0.2809	1.8204
3e	−3.7775	3.4178	0.2925	2.0875
3f	−3.5179	3.5609	0.2808	1.7377
3g	−3.5477	3.4256	0.2919	1.8370
3h	−3.6750	3.5024	0.2855	1.9281
3i	−3.4360	3.6093	0.2770	1.6355
3j	−3.4379	3.5848	0.2789	1.6485
3k	−3.6609	3.5056	0.2852	1.9115
3l	−3.4733	3.6088	0.2771	1.6714
3m	−4.3604	3.6327	0.2771	2.6169
3n	−4.2844	3.6567	0.2735	2.5100
3o	−4.2734	3.4115	0.2931	2.6766
3p	−4.5929	3.6314	0.2753	2.9045
3q	−4.2153	3.4112	0.2931	2.6045
3r	−4.4553	3.6327	0.2753	2.7321
3s	−4.3774	3.6428	0.2745	2.6300
3t	−4.0135	3.5459	0.2820	2.2714
3u	−4.4741	3.9516	0.2530	2.5328
3v	−4.3073	4.0028	0.2498	2.3175
3w	−4.4730	3.7813	0.2644	2.6456
3x	−3.1979	1.9026	0.5256	2.6875

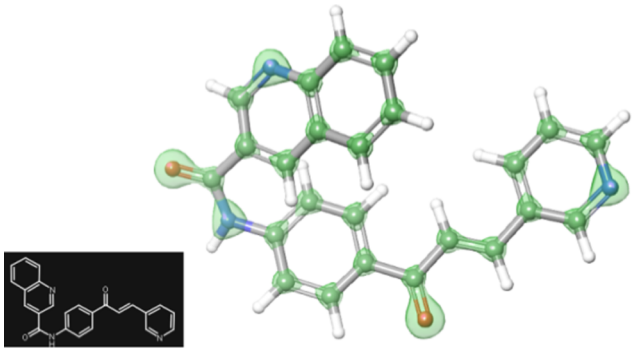

Fig. 4. Fukui functions $(f_k^-) \approx |HOMO|^2$ for the compound **3u**.

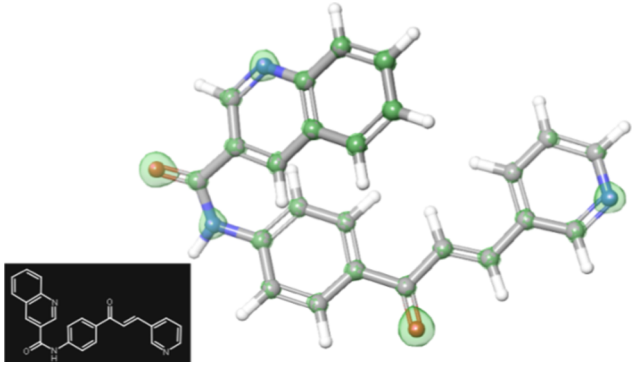

Fig. 5. Fukui functions $(f_k^+) \approx |LUMO|^2$ for the compound **3u**.

the EWG or ERG along with the molecular set.

Analysis *in silico* was made to predict ADME/Tox properties (Table 5). This analysis showed some interesting properties like Log P. This is an important parameter to estimate the lipophilicity of one compound and if it is permeable across the membrane with exception of compound **3m,** compounds **3a–x** are within the range [57,58]. Another interesting parameter is the percent of human oral adsorption because most drugs are administered via oral route. It's known that poor oral

Table 5
Calculated physicochemical descriptors of compounds **3a–x**.

Entry	M.W.	Log P	Log S	PHOA[a]	RO5[b]
3a	385.462	5.265	−6.057	100.0	1
3b	323.391	3.772	−4.314	100.0	0
3c	337.374	3.121	−3.438	100.0	0
3d	311.355	3.945	−4.541	100.0	0
3e	361.363	4.720	−5.673	100.0	0
3f	373.451	4.693	−5.538	100.0	0
3g	283.326	2.920	−3.158	100.0	0
3h	327.810	4.211	−4.933	100.0	0
3i	353.417	3.865	−4.583	100.0	0
3j	383.443	3.910	−4.561	100.0	0
3k	372.261	4.290	−5.054	100.0	0
3l	307.391	4.032	−4.776	100.0	0
3m	522.599	8.340	−9.804	100.0	2
3n	398.457	5.203	−6.072	100.0	1
3o	426.425	3.911	−4.352	100.0	0
3p	374.386	5.568	−6.594	100.0	1
3q	458.510	5.372	−6.648	100.0	1
3r	338.405	5.090	−5.845	100.0	1
3s	366.459	5.742	−7.064	100.0	1
3t	422.439	4.238	−5.872	100.0	0
3u	379.417	3.772	−5.706	96.7	0
3v	378.429	4.722	−6.397	100.0	0
3w	463.922	5.489	−7.818	95.7	1
3x	382.421	3.828	−5.868	100.0	0
*	273.331	1.805	−1.766	90.1	0
**	379.498	4.454	−4.841	100.0	0

[a] Percent human oral absorption.
[b] Rule of Five.
* Galantamine.
** Donepezil.

bioavailability is a problem in therapeutic application, particularly when the drugs have a narrow therapeutic window. This make oral bioavailability one of the key considerations to design and synthetize a new compound [59,60]. Solubility in water (Log S) is an important parameter that must be considered in the design of a possible drug because it has a significant impact on distribution, transport, and bioavailability [61]. Another parameter is cell permeability (PCaco), this is important due to the different barriers that a drug has to cross when it is absorbed through intestinal mucosa [62].

This prediction increases the probability of some compounds having better behaviour in an *in vivo* ADME test, offering the possibility of achieving a possible drug.

3. Experimental

3.1. General information

The ultrasonic irradiation was performed by using a Branson ultrasonic cleaner bath, model 1510, 115v, 1.9 L with a mechanical timer (60 min with continuous hold) and heater switch, 47 kHz. ^{1}H and ^{13}C NMR spectra (400 MHz for proton and 100 MHz for carbon) were recorded on an AM-400 spectrometer (Bruker, Rheinstetten, Germany) using $CDCl_3$ and DMSO-d_6 as solvents. Tetramethylsilane (TMS) was used as an internal standard. IR spectra (KBr pellets, 500–4000 cm^{-1}) were recorded on a NEXUS 670 FT-IR spectrophotometer (Thermo Nicolet, Madison, WI, USA). High-resolution mass spectrometry ESI-MS and ESI-MS/MS analyses were conducted in a high-resolution hybrid quadrupole (Q) and orthogonal time-of-flight (TOF) mass spectrometer (Waters/Micromass Q-TOF micro, Manchester, UK) with a constant nebulizer temperature of 100 °C. Melting points (uncorrected) were measured on an Electrothermal IA9100 melting point apparatus (Stone, Staffs, UK). Reaction progress was monitored by means of thin-layer chromatography using silica gel 60 (Merck, Darmstadt, Germany). All reagents were purchased from either Merck or Sigma Aldrich (St. Louis, MO, USA) and used without further purification. Final purification of

all products for analysis was carried out by recrystallization. GC-MS analyses were performed on a model Trace 1300 GC-MS instrument (Thermo Fisher Scientific, Waltham, MA, USA) equipped with a Rtx-5MS on-column auto injector and a fused silica capillary column (DB-5, 30 m × 0.25 mm ID, 0.25 μm film thickness). Operating conditions were as follows: helium as the carrier gas with a flow rate of 1.5 mL/min; column temperature 40 °C as initial temperature, then increasing at 10 °C/min to 280 °C; injector temperature, 250 °C; volume injected, 1 μL; split ratio, 33.3. MS were recorded in electron ionization (EI) mode with energy of 70 eV. The ion source temperature was 200 °C; 4.00 min solvent cut time. The compounds were identified by comparison with the data held in the NIST 11 Library; data are reported as *m/z* ratio with the relative abundance of the respective peak.

3.2. Acetylcholinesterase assay

The evaluation of enzyme inhibition was carried out applying the Ellman's spectrophotometric method [51]. AChE (from *Electrophorus electricus*) and BuChE (from equine serum), 5,5′-dithio-bis-(2-nitrobenzoic acid (DTNB), acetylthiocholine and butyrylthiocholine iodides were purchased from Sigma-Aldrich. The stock solutions of the test compounds were prepared in 100 μL of DMSO and 900 μL of phosphate buffer (8 mmol/L K_2HPO_4, 2.3 mmol/L NaH_2PO_4, 150 mmol/L NaCl, and 0.05% Tween 20 at pH 7.6). In a 96-well plate, 50 μL of stock solutions were diluted with phosphate buffer to obtain concentrations between 15 and 500 μg/mL for each compound. Enzyme solutions were prepared with buffer to give 0.25 units/mL and 50 μL was added to the plate. After 30 min of incubation, the substrate solution consisting of Na_2HPO_4 (40 mmol/L), acetylthiocholine/butyrylthiocholine (0.24 mmol/L) and DTNB (0.2 mmol/L) was added. The mixture was incubated for another 5 min and the absorption at 405 nm was determined with a Microtiter plate reader (Multiskan EX, Thermo). Each compound concentration was tested in triplicate. The IC_{50} values were calculated by means of regression analysis.

3.3. Kinetic study

For enzymatic kinetic studies of compound **3u**, the enzyme solution was pre-incubated with different substrate concentrations ranging from 9.38×10^{-4} to 0.48 mM. For the determination of the type of inhibition, V_{max} and K_m (Michaelis constant) as well as double reciprocal plots (1/V versus 1/[S] where V = reaction rate and S = substrate concentration) were constructed using Lineweaver–Burk methods. Determinations were made in the absence and presence of **3u**. At least three different concentrations of inhibitor were used in each instance and the experiment was performed in triplicate. Data analysis was carried out with SigmaPlot v10.0 and Enzyme Kinetic v1.3 add-on (Systat Software, Inc, CA, US).

3.4. ADME prediction

The absorption, distribution, metabolism, excretion properties of the compounds, as well as the toxicity were predicted using *QikProp* module from suite Schrödinger [63].

3.5. Computational Details

All the structures included in this study were optimized at B3LYP/6-31G(d) [64] level of theory by using the Gaussian 09 package [65]. We wish to confront the results of model development using the conceptual of DFT (Density Functional Theory). The DFT of chemical reactivity (called conceptual DFT) is used in combination with the molecular quantum similarity approach introduced by Carbo and co-workers. In this, the chemical reactivity descriptors supported in DFT [66–68], like chemical potential (μ)[69–72], hardness (η) [73–75], electrophilicity (ω) [76,77], and local reactivity descriptors like condensed-to-atom Fukui function (f_k^x) [78–80], were used to obtain new insights about the stabilization process in the active site.

The global chemical reactivity like μ shows the tendency of electrons to escape from the electronic cloud. The η represents a measure of the opposition of the electronic cloud to deformation and the ω represents the stabilization energy of the system when it is saturated by electrons from the external environment. These global chemical descriptors can be calculated as follows:

$$\mu = \left(\frac{\partial E}{\partial N}\right)_{v(\boldsymbol{r})} \tag{1}$$

$$\eta = \left(\frac{\partial^2 E}{\partial N^2}\right)_{v(\boldsymbol{r})} \tag{2}$$

where $v(\boldsymbol{r})$ ω is defined as

$$\omega = \frac{\mu^2}{2\eta} = \frac{\chi^2}{2\eta} \tag{3}$$

Using the finite difference approximations in Eqs. (1) and (2), μ and η can be expressed as:

$$\mu = -\frac{I + A}{2} \tag{4}$$

and

$$\eta = I - A \tag{5}$$

Here, I and A are the ionization potential and electron affinity, respectively. I and A were calculated through Koopmans' theorem.

$$\text{where } I = -E_{\text{HOMO}} \tag{6}$$

$$\text{and } A = -E_{\text{LUMO}} \tag{7}$$

The local chemical reactivity through the Fukui functions $f_k^x (x = +, -)$ were computed as follows:

$$f_k^+ = q_k(N+1) - q_k(N) \text{ for nucleophilic attack} \tag{8a}$$

$$f_k^- = q_k(N) - q_k(N-1) \text{ for electrophilic attack} \tag{8b}$$

In these equations, q_k refers to the electron population at k^{th} atomic site in a compound. In this study, we adopted a natural population analysis (NPA) scheme to evaluate atomic charge. Recently, our computational group has been working on new methodologies to understand the non-covalent interactions [81,82].

3.6. Antioxidant activity

3.6.1. Measurement of DPPH radical scavenging activity

The scavenging activities of the compounds were estimated using DPPH as the free radical model according to the method previously described and adapted [83]. Briefly, an aliquot of 1 mL of the tested compound (10–100 μg/mL) and control (2% DMSO final), respectively, were mixed with 2 mL of a methanolic solution of DPPH (0.02 mg/mL). The mixture was shaken vigorously and left to stand at room temperature for 5 min in the absence of light. The mixture was measured spectrophotometrically at 517 nm. The free radical scavenging activity was calculated as the percentage of DPPH decolouration using the following equation:

$$\%\text{scavenging DPPH free radical} = 100 \times (1 - \text{AE/AD})$$

where AE, is the absorbance of the solution after adding the extract and AD is the absorbance of the blank DPPH solution. Ascorbic acid was used as reference compounds with IC_{50} value of 1.5 μg/mL.

3.6.2. Measurement of ABTS radical scavenging activity

The assay was performed according to a published protocol [41]. The stock solution was prepared by mixing equal volumes of 7 mM ABTS solution and 2.45 mM potassium persulfate solution followed by

incubation for 12 h at room temperature in the dark to yield a dark-colored solution containing $ABTS^+$ radicals. A working solution was freshly prepared before each assay by diluting the stock solution by adding 50% methanol for an initial absorbance of about 0.700 (+0.02) at 732 nm at room temperature. Free radical scavenging activity was assessed by mixing 300 μL of different compounds (10–200 μg/mL in respective solvents) with 3.0 mL of ABTS working standard. The decrease in absorbance was measured exactly 1 min after mixing the solution; the final absorbance was noted up to 6 min. Data for each assay was recorded in triplicate. Ascorbic acid, with an IC_{50} value of 28 μg/mL, was used as the positive control. The scavenging activity was estimated based on the percentage of ABTS radicals scavenged by the following formula:

$$\%\text{scavenging} = [(A0-As)/A0] \times 100$$

where A0 is absorption of control, As is absorption of tested compound solution.

3.7. Crystallography

XRD data of **3a** were collected at room temperature using a Bruker Kappa CCD diffractometer. Data collection, data reduction, and cell refinement were done using Bruker Smart, Saintplus, APEX3, respectively. XRD data of **3e** were collected at room temperature using a RIGAKU XTaLAB P200 diffractometer. Data collection, data reduction and cell refinement was done using CrystalClear 2.1 [84]. The program used to refine the crystal structures and prepare materials for publication were SHELXL, Olex2 and PLATON [85–87]. The structures were solved by direct methods and refined with the full-matrix least-squares method on F^2. All H-atoms were positioned geometrically and constrained to ride on their parent atoms. The **3e** compound shows disorder at C3 and F atoms. The F1, F2, and F3 atoms are disordered over two sets of sites. The C3 atom is disordered over two sets of sites and has a refined occupancy ratio of 0.615(9):0.385(11).

3.8. Molecular docking

Molecular docking of the most active compound was done to check the possible interaction modes between Ache and ligands. Molecular docking is a powerful tool usually used in drug-design. Docking was done using grid-base ligand docking with energetics (Glide) contained in Maestro software (Schrödinger Release 2017-1: Maestro, Schrödinger, LLC, New York, NY, 2017). Glide performs a meticulous search of the space available in regards to position, orientation, and conformation for ligands. All these are made through numerous hierarchical filters which allow finding the possible location of ligands in receptor space previously built [88]. This conformational search is made through an algorithm that involves systematic and stochastic methods which perform structural variations of ligands as torsional, translational, and rotational degrees of freedom [89]. Finally, Glide uses a modified score function based on the ChemScore function of Eldridge et al. [90], which estimates the free binding energy of the ligand-receptor complex.

The coordinates of protein were taken from the X-ray crystal structure of AChE-donepezil complex (PDB code 1EVE). This structure was modified with *Protein Preparation Wizard* application of the Maestro module. The grid box was centred on the donepezil with a size of 16 Å × 16 Å × 16 Å. Exploration of large conformational space to look for minimal energy of ligands was made with OPLS2005 force field with a distance-dependent dielectric 2.0 [91]. The Monte Carlo procedure was used for finding the lower energy pose close to the torsional minima.

3.9. Chemistry

3.9.1. N-(4-acetylphenyl)quinoline-3-carboxamide (2t)

A mixture of commercial quinoline-3-carboxylic acid and freshly distilled thionyl chloride was warmed into reflux for 3 h, then cooled to room temperature and evaporated under vacuum to dryness to quantitatively obtain the corresponding chloride acids. This crude material could be used without further purification. A mixture of these chloride acids (1.0 equiv) and 4-aminoacetophenone (1.0 equiv) in toluene (10 mL) was stirred at room temperature for 2 h and then treated with a saturated $NaHCO_3$ solution. The biphasic solution was vigorously stirred for 30 min, then decanted, and finally separated. The collected aqueous phase was extracted with EtOAc (2 × 10 mL). The combined organic layer was dried over Na_2SO_4 and evaporated. The solid was washed with cold water and crude material was crystallized from ethanol.

Yield 90%, white solid; m.p. = 255–257 °C; IR (KBr, cm^{-1}): 3327, 3068, 3001, 1985, 1918, 1844, 1676, 1650, 1597, 1268, 1109, 799; ^1H NMR (400 MHz, DMSO-d_6): 2.55 (s, 3H), 7.71 (t, J = 8.0 Hz, 1H), 7.89 (t, J = 8.0 Hz, 1H), 7.99 (s, 4H), 8.12 (dd, J = 8.0, 12.3 Hz, 2H), 8.99 (s, 1H), 9.37 (s, 1H), 10.90 (bs, 1H); ^{13}C NMR (100 MHz, DMSO-d_6) δ_C: 26.4 (CH_3), 119.5 (2 × CH), 126.3 (C), 127.3 (C), 127.5 (CH), 128.8 (CH), 129.2 (CH), 129.3 (2 × CH), 131.5 (CH), 132.2 (C), 136.2 (CH), 143.4 (C), 148.5 (C), 149.0 (CH), 164.5 (C), 196.5 (C);

General procedure for the preparation and purification of chalcones **3(a–l)**:

A solution of equimolar amounts of 4-(4-Morpholinyl)benzaldehyde **1a** (1 mmol) and acetophenone **2a–s** (1 mmol), using Potassium hydroxide in ethanol (10 mL) as a solvent in an Erlenmeyer, was placed in a water bath and sonicated at room temperature for an appropriate time (10–20 min) until the reaction was completed (the reaction was monitored by TLC). The reaction mixture was then treated with a cold bath and filtered to leave a solid product, which was washed with a hexane to yield pure products **3** (**a–l**). The synthesized compounds with their physical data are listed below.

3.9.2. (E)-3-(4-morpholinophenyl)-1-(4-phenoxyphenyl)prop-2-en-1-one (3a)

Yield: 58% (223.4 mg); yellow solid; mp 202–204 °C; IR (KBr, cm^{-1}): 3120, 2975, 1750, 1654, 1498, 1320, 1201, 758, 660; ^1H NMR (200 MHz, CD_3Cl) 3.25–3.30 (m, 4H), 3.85–3.90 (m, 4H), 6.90 (d, J = 8.0 Hz, 2H), 7.03 (s, 1H), 7.08 (bs, 2H), 7.11–7.13 (m, 1H), 7.27 (s, 1H), 7.36–7.38 (m, 1H), 7.41–7.45 (m, 2H), 7.58 (d, J = 8.0 Hz, 2H), 7.80 (d, J = 16.0 Hz, 1H), 8.03 (d, J = 8.0, 2H); HRMS (ESI, m/z): calculated for $C_{25}H_{23}NO_3$ $[M]^+$ 385.1678 found 385.1662.

3.9.3. (E)-1-(4-methoxyphenyl)-3-(4-morpholinophenyl)prop-2-en-1-one (3b)

Yield: 20% (64.6 mg); yellow solid; mp 154–156 °C; IR (KBr, cm^{-1}): 3097, 2950, 1748, 1598, 1545, 1288, 1220, 1130, 720, 554; ^1H NMR (400 MHz, CD_3Cl) 3.22–3.27 (m, 4H), 3.83–3.87 (m, 7H), 6.92 (dd, J = 16.1 8.9 Hz, 4H), 7.39 (d, J = 15.5 Hz, 1H), 7.55 (d, J = 8.9 Hz, 2H), 7.75 (d, J = 15.5 Hz, 1H), 8.02 (d, J = 8.9 Hz, 2H); HRMS (ESI, m/z): calculated for $C_{20}H_{21}NO_3$ $[M]^+$ 323.1521; found 323.1514.

3.9.4. (E)-1-(benzo[d][1,3]dioxol-5-yl)-3-(4-morpholinophenyl)prop-2-en-1-one (3c)

Yield: 54% (182.0 mg); yellow solid; mp 161–163 °C; IR (KBr, cm^{-1}): 3110, 3050, 2970, 1721, 1689, 1645, 1502, 1272, 1224, 1105, 889, 572; ^1H NMR (400 MHz, CD_3Cl) 3.22–3.27 (m, 4H), 3.82–3.87 (m, 4H), 6.04 (s, 2H), 6.87 (d, J = 9.4 Hz, 3H), 7.34 (d, J = 15.5 Hz, 1H), 7.51–7.52 (m, 2H), 7.57 (s, 1H), 7.62 (dd, J = 8.2,1.7 Hz, 1H), 8.02 (d, J = 15.4 Hz, 1H); GC-MS m/z (rel.int. %): 164 (28), 149 (100), 121 (48), 91 (20); HRMS (ESI, m/z): calculated for $C_{20}H_{19}NO_4$ $[M]^+$ 337.1314 found 337.1323.

*3.9.5. (E)-1-(4-fluorophenyl)-3-(4-morpholinophenyl)prop-2-en-1-one **(3d)***

Yield: 41% (127.6 mg); yellow solid; mp 155–157 °C; IR (KBr, cm^{-1}): 3121, 2962, 1721, 1749, 1695, 1623, 1601, 1502, 1242, 1254, 1112, 1045, 937, 574; ^{1}H NMR (400 MHz, CD_3Cl) 3.24–3.29 (m, 4H), 3.83–3.88 (m, 4H), 6.88 (d, J = 8.8 Hz, 2H), 7.15 (d, J = 8.8 Hz, 2H), 7.34 (d, J = 15.5 Hz, 1H), 7.55 (d, J = 8.8 Hz, 2H), 7.77 (d, J = 15.5 Hz, 1H), 8.02 (dd, J = 8.8, 5.4 Hz, 2H); HRMS (ESI, m/z): calculated for $C_{19}H_{18}FNO_2$ $[M]^+$ = 311.1322 found 311.1325.

*3.9.6. (2E)-3-[4-(morpholin-4-yl)phenyl]-1-[4-(trifluoromethyl)phenyl] prop-2-en-1-one **(3e)***

Yield: 44% (158.9 mg); yellow solid; mp 152–154 °C; IR (KBr, cm^{-1}): 3113, 2987, 1704, 1651, 1532, 1343, 1207, 1003, 954, 825, 551; ^{1}H NMR (400 MHz, CD_3Cl) 3.26–3.31 (m, 4H), 3.84–3.89 (m, 4H), 6.90 (d, J = 8.8 Hz, 2H), 7.32 (d, J = 15.5 Hz, 1H), 7.58 (d, J = 8.8 Hz, 2H), 7.77 (m, 3H), 8.07 (d, J = 8.1 Hz, 2H); HRMS (ESI, m/z): calculated for $C_{20}H_{17}F_3NO_2$ $[M-H]^+$ 360.1212 found 360.1205.

*3.9.7. (E)-1-(6-methoxynaphthalen-2-yl)-3-(4-morpholinophenyl)prop-2-en-1-one **(3f)***

Yield: 20% (74.6 mg); yellow solid; mp 192–194 °C; IR (KBr, cm^{-1}): 3053, 2920, 1741, 1687, 1627, 1574, 1302, 1225, 1142, 1072, 937, 852, 617; ^{1}H NMR (400 MHz, CD_3Cl) 3.24–3.29 (m, 4H), 3.84–3.89 (m, 4H), 3.95 (s, 3H), 6.90 (d, J = 8.8 Hz, 2H), 7.18 (bs, 2H), 7.50 (s, 1H), 7.58–7.65 (m, 3H), 7.86 (dd, J = 8.8, 5.7 Hz, 2H), 8.07 (d, J = 8.8 Hz, 1H); 8.46 (s, 1H); HRMS (ESI, m/z): calculated for $C_{24}H_{23}NO_3$ $[M-H]^+$ 373.1678 found 373.1698.

*3.9.8. (E)-1-(furan-2-yl)-3-(4-morpholinophenyl)prop-2-en-1-one **(3g)***

Yield: 50% (141.6 mg); yellow solid; mp 172–174 °C;IR (KBr, cm^{-1}): 3065, 2995, 1732, 1670, 1650, 1524, 1403, 1265, 1217, 1113, 831, 761; ^{1}H NMR (200 MHz, CD_3Cl) 3.23–3.27 (m, 4H), 3.82–3.87 (m, 4H), 6.55 (dd, J = 3.5, 1.7 Hz, 1H), 6.87 (d, J = 8.0 Hz, 2H), 7.27 (d, J = 3.5 Hz, 1H), 7.33 (s, 1H), 7.54 (bs, 1H), 7.58–7.62 (m, 2H), 7.82(d, J = 16.0 Hz, 1H); HRMS (ESI, m/z): calculated for $C_{17}H_{17}NO_3$ $[M]^+$ 283.1208 found 283.1212.

*3.9.9. (E)-1-(4-chlorophenyl)-3-(4-morpholinophenyl)prop-2-en-1-one **(3h)***

Yield: 77% (251.9 mg); yellow solid; mp 170–172 °C; IR (KBr, cm^{-1}): 3087, 2904, 1741, 1615, 1523, 1207, 1108, 1033, 871, 632, 584; ^{1}H NMR (200 MHz, CD_3Cl) 3.24–3.28 (m, 4H), 3.82–3.87 (m, 4H), 6.88 (d, J = 8.8 Hz, 2H), 7.32 (d, J = 15.5 Hz, 1H), 7.44 (d, J = 8.6 Hz, 2H) 7.55 (d, J = 8.9 Hz, 2H), 7.76(d, J = 15.5 Hz, 1H), 7.93 (d, J = 8.9, 2H); GC-MS m/z (rel.int. %):191(24), 154 (22), 134 (10), 133 (100), 132 (80).

*3.9.10. (E)-1-(3,4-dimethoxyphenyl)-3-(4-morpholinophenyl)prop-2-en-1-one **(3i)***

Yield: 34% (120.1 mg); yellow solid; mp 158–160 °C; IR (KBr, cm^{-1}): 3101, 2983, 1733, 1678, 1662, 1587, 1492, 1304, 1254, 1197, 1073, 996, 714, 558; ^{1}H NMR (400 MHz, CD_3Cl); 3.03–3.06 (m, 4H), 3.64–3.66 (m, 4H), 3.75–3.76 (m, 6H) 6.67–6.72 (m, 3H), 7.21 (d, J = 16.0 Hz, 1H) 7.35 (d, J = 8.0 Hz, 2H), 7.42 (bs, 1H), 7.47(d, J = 8.0, 1H), 7.57(d, J = 16.0 Hz, 1H); HRMS (ESI, m/z): calculated for $C_{21}H_{23}NO_4$ $[M]^+$ 353.1627 found 353.1626.

*3.9.11. (E)-3-(4-morpholinophenyl)-1-(3,4,5-trimethoxyphenyl)prop-2-en-1-one **(3j)***

Yield: 42% (160.9 mg); yellow solid; mp 187–189 °C; IR (KBr, cm^{-1}): 3091, 2961, 1733, 1667, 1652, 1498, 1230, 1175, 998, 885, 673; ^{1}H NMR (200 MHz, CD_3Cl) 3.25–3.29 (m, 4H), 3.84–3.89 (m, 4H), 3.93 (s, 3H), 3.95 (s, 6H), 6.90 (d, J = 8.0 Hz, 2H), 7.27 (s, 2H), 7.33 (d, J = 16.0 Hz, 1H), 7.58 (d, J = 8.0 Hz, 2H), 7.80 (d, J = 16.0 Hz, 1H); HRMS (ESI, m/z): calculated for $C_{22}H_{25}NO_5$ $[M]^+$ 383.1733 found 383.1718.

*3.9.12. (E)-1-(4-bromophenyl)-3-(4-morpholinophenyl)prop-2-en-1-one **(3k)***

Yield: 89% (330.2 mg); yellow solid; mp 182–184 °C; IR (KBr, cm^{-1}): 3068, 3001, 1742, 1647, 1522, 1401, 1265, 1218, 822, 793, 672, 575; ^{1}H NMR (400 MHz, CD_3Cl) 3.25–3.28 (m, 4H), 3.84–3.87 (m, 4H), 6.88 (d, J = 8.0 Hz, 2H), 7.32 (d, J = 16.0 Hz, 1H), 7.56 (d, J = 8.0 Hz, 2H), 7.62 (d, J = 8.0 Hz, 2H), 7.77 (d, J = 16.0 Hz, 1H), 7.87 (d, J = 8.0 Hz, 2H); HRMS (ESI, m/z): calculated for $C_{19}H_{18}BrNO_2$ $[M]^+$ 371.0521 found 371.0515.

*3.9.13. (E)-3-(4-morpholinophenyl)-1-(p-tolyl)prop-2-en-1-one **(3l)***

Yield: 30% (92.1 mg); yellow solid; mp 140–142 °C; IR (KBr, cm^{-1}): 3057, 2936, 1748, 1653, 1564, 1298, 1219, 1134, 1002, 894, 684, 581; ^{1}H NMR (400 MHz, CD_3Cl) 2.42 (s, 3H), 3.24–3.26 (m, 4H), 3.84–3.86 (m, 4H), 6.88 (d, J = 8.0 Hz, 2H), 7.28 (d, J = 8.0 Hz, 2H), 7.38 (d, J = 16.0 Hz, 1H), 7.56 (d, J = 8.0 Hz, 2H), 7.75 (d, J = 16.0 Hz, 1H), 7.91 (d, J = 8.0, 2H); HRMS (ESI, m/z): calculated for $C_{20}H_{21}NO_2$ $[M]^+$ 307.1572 found 307.1590.

*3.9.14. (2E,2′E)-3,3′-(1,4-phenylene)bis(1-(4-phenoxyphenyl)prop-2-en-1-one) **(3m)***

Yield: 68% (355.4 mg); yellow solid; mp 183–185 °C; IR-FT (KBr, cm^{-1}): 3064, 3038, 3007, 1661, 1591, 1489, 1416, 1337, 1225, 1168, 1024, 979, 870; ^{1}H NMR (400 MHz, $CDCl_3$) δ 7.19–7.29 (m, 8H), 7.37 (t, J = 7.9 Hz, 2H), 7.57 (t, J = 7.9 Hz, 4H), 7.73 (d, J = 15.7 Hz, 2H), 7.84 (s, 4H), 7.97 (d, J = 15.7 Hz, 2H), 8.20 (d, J = 8.7 Hz, 4H); ^{13}C NMR (100 MHz, $CDCl_3$) δ 117.4 (4 × CH), 120.1 (4 × CH), 122.7 (2 × CH), 124.6 (2 × CH), 128.8 (4 × CH), 130.0 (4 × CH), 130.8 (4 × CH), 132.5 (2 × C), 136.8 (2 × C), 143.1 (2 × CH), 155.4 (2 × C), 161.9 (2 × C), 188.4 (2 × C); HRMS (ESI, m/z): calculated for $C_{36}H_{26}O_4$ $[M]^+$ 522.1831 found 522.1832.

*3.9.15. (2E,2′E)-3,3′-(1,4-phenylene)bis(1-(4-methoxyphenyl)prop-2-en-1-one) **(3n)***

Yield: 68% (270.9 mg); yellow solid; mp 245–247 °C; IR-FT (KBr, cm^{-1}): 3077, 2981, 2931, 2834, 1659, 1609, 1570, 1507, 1424, 1340, 1288, 1262, 1228, 1175, 1113, 987, 812; ^{1}H NMR (400 MHz, DMSO-d_6) δ 3.88 (s, 6H), 7.10 (d, J = 8.8 Hz, 4H), 7.75 (d, J = 15.6, Hz, 2H), 7.98 (s, 4H), 8.04 (d, J = 15.6 Hz, 2H), 8.20 (d, J = 8.8 Hz, 4H); ^{13}C NMR (100 MHz, DMSO-d_6) δ 54.9 (2 × CH_3), 113.5 (4 × CH), 123.3 (2 × CH), 128.1 (4 × CH), 129.9 (4 × CH), 130.3 (2 × C), 136.1 (2 × C), 141.0 (2 × CH), 162.7 (2 × C), 187.2 (2 × C); HRMS (ESI, m/z): calculated for $C_{26}H_{22}O_4$ $[M]^+$ 398.1518 found 398.1514.

*3.9.16. (2E,2′E)-3,3′-(1,4-phenylene)bis(1-(benzo[d][1,3]dioxol-5-yl) prop-2-en-1-one) **(3o)***

Yield: 58% (247.3 mg); yellow solid; mp 254–256 °C; IR-FT (KBr, cm^{-1}): 3088, 3033, 3921, 1661, 1599, 1502, 1444, 1332, 1251, 1115, 1045, 925, 815; ^{1}H NMR (400 MHz, DMSO-d_6) δ 6.17 (s, 4H), 7.11 (d, J = 8.2 Hz, 2H), 7.69 (d, J = 1.3 Hz, 2H), 7.74 (d, J = 15.6, Hz, 2H), 7.90 (d, J = 8.2 Hz, 2H), 7.98 (s, 4H), 8.02 (d, J = 15.6 Hz, 2H); ^{13}C NMR (100 MHz, DMSO-d_6) δ 102.6 (2 × CH_2), 108.4 (2 × CH), 125.9 (2 × CH), 129.8 (4 × CH), 130.3 (4 × CH), 137.4 (2 × C), 140.9 (2 × C), 142.2 (2 × CH), 148.5 (2 × C), 152.3 (2 × C), 193.1 (2 × C); HRMS (ESI, m/z): calculated for $C_{26}H_{22}O_4$ $[M]^+$ 426.1103 found 426.1168.

*3.9.17. (2E,2′E)-3,3′-(1,4-phenylene)bis(1-(4-fluorophenyl)prop-2-en-1-one) **(3p)***

Yield: 61% (228.4 mg); yellow solid; mp 238–240 °C; IR-FT (KBr, cm^{-1}): 3075, 3028, 1660, 1598, 1504, 1416, 1346, 1164, 1024, 975; ^{1}H NMR (400 MHz, DMSO-d_6) δ 7.48 (t, J = 8.6 Hz, 4H), 7.85 (d, J = 15.6 Hz, 2H), 8.06 (s, 4H), 8.12 (d, J = 15.6 Hz, 2H), 8.32–8.38 (m, 4H); ^{13}C NMR (100 MHz, DMSO-d_6) δ 115.9 (2 × CH), 116.1 (2 × CH),

124.4 (2 × CH), 129.5 (4 × CH), 131.7 (2 × CH), 131.7 (2 × CH), 137.3 (2 × C), 143.3 (2 × CH), 164.3 (2 × C), 166.5 (2 × C), 188.9 (2 × C); HRMS (ESI, *m/z*): calculated for $C_{24}H_{16}F_2O_2$ $[M]^+$ 374.1118 found 374.3896.

*3.9.18. (2E,2′E)-3,3′-(1,4-phenylene)bis(1-(3,4-dimethoxyphenyl)prop-2-en-1-one) (**3q**)*

Yield: 68% (311.8 mg); yellow solid; mp 218–220 °C; IR-FT (KBr, cm^{-1}): 3085, 3017, 2962, 2934, 2834, 1651, 1599, 1583, 1518, 1418, 1332, 1149, 1024, 985, 815; ^{1}H NMR (400 MHz, $CDCl_3$) δ 3.98 (s, 12H), 6.94 (d, J = 8.4 Hz, 2H), 7.60 (d, J = 15.6 Hz, 2H), 7.64 (d, J = 1.7 Hz, 2H), 7.69 (s, 5H), 7.71 (d, J = 1.7 Hz, 1H), 7.81 (d, J = 15.6 Hz, 2H); ^{13}C NMR (100 MHz, $CDCl_3$) δ 56.0 (2 × CH_3), 56.1 (2 × CH_3), 109.9 (2 × CH), 110.7 (2 × CH), 122.5 (2 × CH), 123.0 (2 × CH), 128.8 (4 × CH), 131.1 (2 × C), 136.8 (2 × C), 142.7 (2 × CH), 149.3 (2 × C), 153.4 (2 × C), 188.2 (2 × C); HRMS (ESI, *m/z*): calculated for $C_{28}H_{26}O_6$ $[M]^+$ 458.1729 found 458.1720.

*3.9.19. (2E,2′E)-3,3′-(1,4-phenylene)bis(1-phenylprop-2-en-1-one) (**3r**)*

Yield: 73% (247.0 mg); yellow solid; mp 191–193 °C; IR-FT (KBr, cm^{-1}): 3054, 3038, 1659, 1646, 1416, 1335, 1222, 1037, 1024, 979, 828, 770; ^{1}H NMR (400 MHz, $CDCl_3$) δ 7.52 (dd, J = 10.3, 4.6 Hz, 4H), 7.55 –7.63 (m, 4H), 7.69 (s, 4H), 7.81 (d, J = 15.7 Hz, 2H), 8.04 (d, J = 7.1 Hz, 4H); ^{13}C NMR (100 MHz, $CDCl_3$) δ 123.0 (2 × CH), 128.5 (4 × CH), 128.6 (4 × CH), 128.9 (4 × CH), 132.9 (2 × CH), 136.8 (2 × C), 138.0 (2 × C), 143.5 (2 × CH), 190.2 (2 × C); HRMS (ESI, *m/z*): calculated for $C_{24}H_{18}O_2$ $[M]^+$ 338.1307 found 338.4094.

*3.9.20. (2E,2′E)-3,3′-(1,4-phenylene)bis(1-(p-tolyl)prop-2-en-1-one) (**3s**)*

Yield: 82% (300.5 mg); yellow solid; mp 234–236 °C; IR-FT (KBr, cm^{-1}): 3033, 2921, 1659, 1612, 1603, 1421, 1337, 1230, 1181, 1037, 985, 812; ^{1}H NMR (400 MHz, DMSO-d_6) δ 2.42 (s, 6H), 7.40 (d, J = 7.4 Hz, 4H), 7.76 (d, J = 15.6 Hz, 2H), 7.98 (s, 4H), 8.03 (d, J = 15.6 Hz, 2H), 8.10 (d, J = 7.6 Hz, 4H); ^{13}C NMR (100 MHz, DMSO-d_6) δ 20.8 (2 × CH_3), 124.1 (2 × C), 128.3 (4 × CH), 128.8 (4 × CH), 129.1 (4 × CH), 135.5 (2 × C), 142.2 (4 × CH), 143.1 (2 × C), 189.2 (2 × C); HRMS (ESI, *m/z*): calculated for $C_{26}H_{22}O_2$ $[M]^+$ 366.1620 found 366.1649.

*3.9.21. (E)-N-(4-(3-(benzo[d][1,3]dioxol-5-yl)acryloyl)phenyl)quinoline-3-carboxamide (**3t**)*

Yield 92% (388.6 mg); yellow solid; m.p. = 237–239 °C; IR (KBr, cm^{-1}): 3334, 2917, 1670, 1595, 1528, 1499, 1534, 1245, 1025, 920, 819, 755; ^{1}H NMR (400 MHz, DMSO-d_6): 6.10 (s, 2H),6.99 (d, J = 8.0 Hz,1H), 7.33 (d, J = 8.0 Hz, 1H), 7.66 (s, 1H), 7.69–7.72 (m, 2H), 7.83 (s, 1H), 7.88–7.90 (m, 1H), 8.01 (d, J = 8.0 Hz, 2H), 8.13 (dd, J = 8.0, 16.8 Hz, 2H), 8.21 (d, J = 8.0 Hz, 2H), 9.00 (s, 1H), 9.39 (s, 1H), 10.93 (bs, 1H); ^{13}C NMR (100 MHz, DMSO-d_6) δ_C: 102.0 (CH_2), 107.3 (CH), 108.9 (CH), 120.7 (CH), 121.7 (CH), 125.9 (CH), 127.3 (C), 127.4 (CH), 129.1 (2 × CH), 129.5 (2 × CH), 130.0 (2 × CH), 130.9 (CH), 135.9 (CH), 143.0 (CH), 148.5 (C), 148.6 (C), 149.7 (C), 150.8 (C), 165.9 (C), 187.4 (C); HRMS (ESI, *m/z*): calculated for $C_{26}H_{19}N_2O_4$ $[M+H]^+$ 423.1345; found 423.1342.

*3.9.22. (E)-N-(4-(3-(pyridin-3-yl)acryloyl)phenyl)quinoline-3-carboxamide (**3u**)*

Yield 77% (292.1 mg); yellow solid, mp 270–272 °C; IR (KBr, cm^{-1}):3307, 3040, 1673, 1659, 1600, 1532, 1473, 1338, 1225, 1175, 1028, 784, 677, 576; ^{1}H NMR (400 MHz, DMSO-d_6): δ_H = 7.50 (m, 1H), 7.75 (m, 2H), 7.91 (t, J = 7.6 Hz, 1H), 8.04 (d, J = 8.3 Hz, 2H), 8.14 (m, 3H), 8.26 (d, J = 8.3 Hz, 2H), 8.36 (t, J = 7.8 Hz, 1H), 8.62 (m, 1H), 9.01 (s, 1H), 9.03 (s, 1H), 9.38 (s, 1H), 10.95 (bs, 1H); ^{13}C NMR (100 MHz, DMSO-d_6) δ_C: 120.1 (2 × CH), 124.3 (CH), 124.4 (CH), 126.8 (C), 127.7 (C), 128.0 (CH), 129.3 (CH), 129.7 (CH), 130.4 (2 × CH), 131.1 (C), 132.0 (CH), 133.1 (C), 135.5 (CH), 136.8 (CH), 140.5 (CH), 144.1 (C), 149.1 (C), 149.5 (CH), 150.8 (CH), 151.4 (CH), 165.1 (C), 187.8 (C); HRMS (ESI, *m/z*): calculated for $C_{24}H_{17}N_3O_2$ $[M]^+$ 379.1321 found 379.1320.

*3.9.23. N-(4-cinnamoylphenyl)quinoline-3-carboxamide (**3v**)*

Yield: 53% (200.6 mg); yellow solid, mp 235–237 °C; IR (KBr, cm^{-1}): 3302, 3039, 1673, 1589, 1519, 1326, 1227, 1166, 1036, 972, 764; ^{1}H NMR (400 MHz, DMSO-d_6): δ_H = 7.46 (m, 3H), 7.74 (m, 2H), 7.90 (m, 3H), 7.98 (d, J = 15.6 Hz, 1H), 8.04 (d, J = 8.0 Hz, 2H), 8.14 (dd, J = 8.0, 15.9 Hz, 1H), 8.24 (d, J = 8.0 Hz, 2H), 9.0 (s, 1H), 9.38 (s, 1H), 10.93 (bs, 1H); HRMS (ESI, *m/z*): calculated for $C_{25}H_{18}N_2O_2$ $[M]^+$ 378.1368 found 378.1369.

*3.9.24. (E)-N-(4-(3-(2-chloroquinolin-3-yl)acryloyl)phenyl)quinoline-3-carboxamide (**3w**)*

Yield 68% (315.5 mg); yellow solid, mp 258–260 °C; IR (KBr, cm^{-1}): 3336, 3057, 1656, 1600, 1521, 1405, 1318, 1220, 1178, 789, 593; ^{1}H NMR (400 MHz, DMSO-d_6): δ_H = 7.66 (t, J = 8.0 Hz, 1H), 7.73 (t, J = 8.0 Hz, 1H), 7.83 (t, J = 8.0 Hz, 2H), 7.89 (m, 2H), 7.99 (d, J = 8.0 Hz, 1H), 8.05 (d, J = 8.0 Hz, 1H), 8.07 (m, 4H), 8.16 (d, J = 8.0 Hz, 2H), 8.22 (d, J = 15.7 Hz, 1H), 8.94 (s, 1H), 9.28 (s, 1H), 9.51 (s, 1H); HRMS (ESI, *m/z*): calculated for $C_{28}H_{18}ClN_3O_2$ $[M]^+$ 463.1088 found 463.1083.

*3.9.25. (E)-N-(4-(3-(1-methyl-1H-imidazol-2-yl)acryloyl)phenyl) quinoline-3-carboxamide (**3x**)*

Yield 71% (271.5 mg), yellow solid, mp 244–246 °C; IR (KBr, cm^{-1}):3264, 2923, 1676, 1653, 1569, 1412, 1334, 1265, 1025, 918, 793, 755; ^{1}H NMR (400 MHz, DMSO-d_6): 6.11 (s, 1H), 6.56 (d, J = 8.6 Hz, 1H), 6.74 (s, 1H), 7.57 (m, 1H), 7.65 (d, J = 8.6 Hz, 2H), 7.72 (m, 1H), 7.82 (d, J = 8.0 Hz, 1H), 8.00 (d, J = 8.0 Hz, 2H), 8.35 (bs, 3H), 8.65 (s, 1H), 9.34 (s, 1H); HRMS (ESI, *m/z*): calculated for $C_{23}H_{18}N_4O_2$ $[M]^+$ 382.1430 found 382.1436.

4. Conclusion

In conclusion, a set of chalcone and bis-chalcone derivatives have been synthesized under ultrasonication conditions via Claisen-Schmidt condensation with KOH in ethanol at room temperature. The structures of the compounds were characterized on the basis of NMR, IR, Single-crystal XRD, and MS. These products were evaluated as potential AChE inhibitors. Most of these compounds showed selectivity against AChE. Compounds **3p, 3q, 3u, and 3v** were significantly *in vitro* active with IC_{50} values of 40.48, 27.41, 7.50, and 12.58 μM, respectively. The kinetic study of compound **3u** showed mixed-type inhibition against AChE. On the other hand, compounds **3o** and **3p** showed a moderated antioxidant capacity compared with the ascorbic acid used as reference. The modelling study of compounds **3p**, **3q**, **3u**, and **3v** showed the same interaction of Donepezil with the residues Trp84, Phe330, and Trp279. The pharmacokinetic profile of these compounds was investigated using a computational method, showing an interesting potential in the design of new compounds with pharmaceutical application.

Declaration of Competing Interest

There are no conflicts to declare.

Acknowledgements

This research was supported by a FONDECYT project number 1150712, PIEI QUIMBIO, project, Utalca. EP and MG give thanks to the CONICYT scholarship No. 63140046. LPP is grateful for the CONICYT scholarship associated with the folio N° 63130155; The authors of the present investigation are grateful for PIEI QUIMBIO Project, Universidad de Talca, Chile.

Appendix A. Supplementary material

Supplementary data to this article can be found online at https://doi.org/10.1016/j.bioorg.2019.103034.

References

[1] G. Giaccone, B. Pedrotti, A. Migheli, L. Verga, J. Perez, G. Racagni, M.A. Smith, G. Perry, L. De Gioia, C. Selvaggini, M. Salmona, J. Ghiso, B. Frangione, K. Islam, O. Bugiani, F. Tagliavini, Am. J. Pathol. 148 (1996) 79–87.
[2] M.T.H. Khan, N. Biotechnol. 25 (2009) 331–346.
[3] M. Pohanka, Exp. Opin. Ther. Pat. 22 (2012) 871–886.
[4] P. Singh, A. Anand, V. Kumar, Eur. J. Med. Chem. 85 (2014) 758–777.
[5] Y.-M. Lin, Y. Zhou, M.T. Flavin, L.-M. Zhou, W. Nie, F.-C. Chen, Bioorg. Med. Chem. 10 (2002) 2795–2802.
[6] R. Wen, H.-N. Lv, Y. Jiang, P.-F. Tu, Phytochemistry 149 (2018) 56–63.
[7] L.-M. Zhao, H.-S. Jin, L.-P. Sun, H.-R. Piao, Z.-S. Quan, Bioorg. Med. Chem. Lett. 15 (2005) 5027–5029.
[8] A. El Maatougui, M. Yáñez, A. Crespo, N. Fraiz, A. Coelho, E. Raviña, R. Laguna, E. Cano, M.I. Loza, J. Brea, H. Gutiérrez de Terán, E. Sotelo, ChemistrySelect 2 (2017) 4920–4933.
[9] M. Liu, P. Wilairat, S.L. Croft, A.L.-C. Tan, M.-L. Go, Bioorg. Med. Chem. 11 (2003) 2729–2738.
[10] C. Gutteridge, J. Vo, C. Tillett, J. Vigilante, J. Dettmer, S. Patterson, K. Werbovetz, J. Capers, D. Nichols, A. Bhattacharjee, L. Gerena, Med. Chem. (Los. Angeles) 3 (2007) 115–119.
[11] H. Aryapour, G.H. Riazi, S. Ahmadian, A. Foroumadi, M. Mahdavi, S. Emami, Pharm. Biol. 50 (2012) 1551–1560.
[12] P. Boeck, C.A. Bandeira Falcão, P.C. Leal, R.A. Yunes, V.C. Filho, E.C. Torres-Santos, B. Rossi-Bergmann, Bioorg. Med. Chem. 14 (2006) 1538–1545.
[13] S. Mudaliar, K.H. Chikhalia, N.K. Shah, Lett. Drug Des. Discov. 13 (2016) 818–823.
[14] J.N. Domínguez, C. León, J. Rodrigues, N. Gamboa de Domínguez, J. Gut, P.J. Rosenthal, J. Med. Chem. 48 (2005) 3654–3658.
[15] V. Kotra, S. Ganapaty, S.R. Adapa, ChemInform 41 (2010) 1109–1116.
[16] M. Sharma, V. Chaturvedi, Y.K. Manju, S. Bhatnagar, K. Srivastava, S.K. Puri, P.M.S. Chauhan, Eur. J. Med. Chem. 44 (2009) 2081–2091.
[17] M.I. Abdullah, A. Mahmood, M. Madni, S. Masood, M. Kashif, Bioorg. Chem. 54 (2014) 31–37.
[18] R. Abonia, D. Insuasty, J. Castillo, B. Insuasty, J. Quiroga, M. Nogueras, J. Cobo, Eur. J. Med. Chem. 57 (2012) 29–40.
[19] N.P. de Sá, P.S. Cisalpino, L.C. Tavares, L. Espíndola, B.M. Borelli, P.J.S. Barbeira, G.de M. Cardoso Perdigão, E.M. Souza-Fagundes, C.A. Rosa, M.G. Pizzolatti, S. Johann, J. Antibiot. (Tokyo) 70 (2017) 277–284.
[20] A. Hameed, M.I. Abdullah, E. Ahmed, A. Sharif, A. Irfan, S. Masood, Bioorg. Chem. 65 (2016) 175–182.
[21] K.V. Sashidhara, S.R. Avula, V. Mishra, G.R. Palnati, L.R. Singh, N. Singh, Y.S. Chhonker, P. Swami, R.S. Bhatta, G. palit, Eur. J. Med. Chem. 89 (2015) 638–653.
[22] D.K. Mahapatra, S.K. Bharti, V. Asati, Eur. J. Med. Chem. 101 (2015) 496–524.
[23] D.N. Dhar, The Chemistry of Chalcones and Related Compounds, Wiley, 1981.
[24] M. Climent, A. Corma, S. Iborra, A. Velty, J. Catal. 221 (2004) 474–482.
[25] R. Ballini, G. Bosica, M. Ricciutelli, R. Maggi, G. Sartori, R. Sartorio, P. Righi, Green Chem. 3 (2001) 178–180.
[26] S. Sebti, A. Solhy, R. Tahir, S. Boulaajaj, J.A. Mayoral, J.M. Fraile, A. Kossir, H. Oumimoun, Tetrahedr. Lett. 42 (2001) 7953–7955.
[27] A. Fuentes, J.M. Marinas, J.V. Sinisterra, Tetrahedr. Lett. 28 (1987) 4541–4544.
[28] M.J. Climent, A. Corma, S. Iborra, J. Primo, J. Catal. 151 (1995) 60–66.
[29] S. Saravanamurugan, M. Palanichamy, B. Arabindoo, V. Murugesan, J. Mol. Catal. A Chem. 218 (2004) 101–106.
[30] Peter W. Cains, A. Peter, D. Martin, C.J. Price, Org. Process Res. Dev. 2 (1998) 34–48.
[31] J.R. Dimmock, D.W. Elias, M.A. Beazely, N.M. Kandepu, Curr. Med. Chem. 6 (1999) 1125–1149.
[32] R. Cella, H.A. Stefani, Tetrahedron 65 (2009) 2619–2641.
[33] F. de Campos-Buzzi, P. Padaratz, A.V. Meira, R. Corrêa, R.J. Nunes, V. Cechinel-Filho, Molecules 12 (2007) 896–906.
[34] S. Vogel, S. Ohmayer, G. Brunner, J. Heilmann, Bioorg. Med. Chem. 16 (2008) 4286–4293.
[35] H.-Y. Qiu, P.-F. Wang, Z. Li, J.-T. Ma, X.-M. Wang, Y.-H. Yang, H.-L. Zhu, Pharmacol. Res. 104 (2016) 86–96.
[36] P.-F. Wang, H.-Y. Qiu, J.-T. Ma, X.-Q. Yan, H.-B. Gong, Z.-C. Wang, H.-L. Zhu, RSC Adv. 5 (2015) 24997–25005.
[37] V. Kanagarajan, M. Ezhilarasi, M. Gopalakrishnan, Org. Med. Chem. Lett. 1 (2011) 8.
[38] V. Kanagarajan, M.R. Ezhilarasi, M. Gopalakrishnan, J. Enzyme Inhib. Med. Chem. 26 (2011) 498–505.
[39] N. El-Rayyes, A.J.A. Al-Johary, J. Chem. Eng. Data 30 (1985) 500–502.
[40] C.S. Chidan Kumar, C.K. Quah, S. Chandraju, N.K. Lokanath, S. Naveen, M. Abdoh, IUCrData 2 (2017) x170238.
[41] S. Khwaja, K. Fatima, M. Hasanain, C. Behera, A. Kour, A. Singh, S. Luqman, J. Sarkar, D. Chanda, K. Shanker, A.K. Gupta, D.M. Mondhe, A.S. Negi, Eur. J. Med. Chem. 151 (2018) 51–61.
[42] W.T.A. Harrison, H.J. Ravindra, M.R. Suresh Kumar, S.M. Dharmaprakash, Acta Crystallogr. Sect. E Struct. Reports Online 63 (2007) o3067–o3067.
[43] W.T.A. Harrison, H.J. Ravindra, M.R. Suresh Kumar, S.M. Dharmaprakash, Acta Crystallogr. Sect. E Struct. Reports Online 63 (2007) o3068–o3068.
[44] F. Chen, F.-M. Liu, Z.-Q. Dong, J. Heterocycl. Chem. 51 (2014) 1764–1769.
[45] J.-G. Shao, J.-F. Zhou, C.-Q. Liu, Q. Zhong, Org. Prep. Proced. Int. 25 (1993) 581–583.
[46] M.B. Gürdere, O. Özbek, M. Ceylan, Synth. Commun. 46 (2016) 322–331.
[47] E. Winter, P. Devantier Neuenfeldt, L.D. Chiaradia-Delatorre, C. Gauthier, R.A. Yunes, R.J. Nunes, T.B. Creczynski-Pasa, A. Di Pietro, J. Med. Chem. 57 (2014) 2930–2941.
[48] C.-Y. Cai, L. Rao, Y. Rao, J.-X. Guo, Z.-Z. Xiao, J.-Y. Cao, Z.-S. Huang, B. Wang, Eur. J. Med. Chem. 130 (2017) 51–59.
[49] D. Cremer, J.A. Pople, J. Am. Chem. Soc. 97 (1975) 1354–1358.
[50] F.H. Allen, D.G. Watson, L. Brammer, A.G. Orpen, R. Taylor, Int. Tables Crystallogr, first ed., International Union of Crystallography, Chester, England, 2006, pp. 790–811.
[51] G.L. Ellman, K.D. Courtney, V. Andres, R.M. Featherstone, Biochem. Pharmacol. 7 (1961) 88–95.
[52] Y. Duarte, A. Fonseca, M. Gutiérrez, F. Adasme-Carreño, C. Muñoz-Gutierrez, J. Alzate-Morales, L. Santana, E. Uriarte, R. Álvarez, M.J. Matos, ChemistrySelect 4 (2019) 551–558.
[53] Y.A. Rodríguez, M. Gutiérrez, D. Ramírez, J. Alzate-Morales, C.C. Bernal, F.M. Güiza, A.R. Romero Bohórquez, Chem. Biol. Drug Des. 88 (2016) 498–510.
[54] G. Kryger, I. Silman, J.L. Sussman, Structure 7 (1999) 297–307.
[55] R.N. Gacche, N.A. Dhole, S.G. Kamble, B.P. Bandgar, J. Enzyme Inhib. Med. Chem. 23 (2008) 28–31.
[56] J. Chu, C.-L. Guo, Arch. Pharm. (Weinheim) 349 (2016) 63–70.
[57] Y. Sakuratani, K. Kasai, Y. Noguchi, J. Yamada, QSAR Comb. Sci. 26 (2007) 109–116.
[58] E.S. Souza, L. Zaramello, C.A. Kuhnen, B. da, S. Junkes, R.A. Yunes, V.E.F. Heinzen, Int. J. Mol. Sci. 12 (2011) 7250–7264.
[59] T. Hou, J. Wang, W. Zhang, X. Xu, J. Chem. Inf. Model. 47 (2007) 208–218.
[60] A. El-Kattan, M. Varm, Top. Drug Metab. InTech, 2012.
[61] T.J. Hou, K. Xia, W. Zhang, X.J. Xu, J. Chem. Inf. Comput. Sci. 44 (2004) 266–275.
[62] P. Artursson, J. Karlsson, Biochem. Biophys. Res. Commun. 175 (1991) 880–885.
[63] W.L. Jorgensen, Schrödinger LLC, New York, 2006.
[64] A.D. Becke, J. Chem. Phys. 107 (1998) 8554.
[65] Frisch, G. Trucks, H. Schlegel, G. Scuseria, M. Robb, J. Cheeseman, J. Montgomery, T. Vreven, K. Kudin, J. Burant, J. Millam, S. Iyengar, J. Tomasi, V. Barone, B. Mennucci, M. Cossi, G. Scalmani, N. Rega, G. Petersson, H. Nakatsuji, M. Hada, M. Ehara, K. Toyota, R. Fukuda, J. Hasegawa, M. Ishida, T. Nakajima, Y. Honda, O. Kitao, H. Nakai, M. Klene, X. Li, J. Knox, H. Hratchian, J. Cross, V. Bakken, C. Adamo, J. Jaramillo, R. Gomperts, R. Stratmann, O. Yazyev, A. Austin, R. Cammi, C. Pomelli, J. Ochterski, P. Ayala, K. Morokuma, G. Voth, P. Salvador, J. Dannenberg, V. Zakrzewski, S. Dapprich, A. Daniels, M. Strain, O. Farkas, D. Malick, A. Rabuck, K. Raghavachari, J. Foresman, J. Ortiz, Q. Cui, A. Baboul, S. Clifford, J. Cioslowski, B. Stefanov, G. Liu, A. Liashenko, P. Piskorz, I. Komaromi, R. Martin, D. Fox, T. Keith, A. Laham, C. Peng, A. Nanayakkara, M. Challacombe, P. Gill, B. Johnson, W. Chen, M. Wong, C. Gonzalez, J. Pople, Gaussian 09, Gaussian Inc., 2009.
[66] Chemical Reactivity Theory: A Density Functional View, CRC Press/Taylor & Francis, Boca Raton, 2009.
[67] P. Geerlings, F. De Proft, W. Langenaeker, Chem. Rev. 103 (2003) 1793–1874.
[68] J.-L. Calais, Int. J. Quant. Chem. 47 (1993) 101–101.
[69] H.J. Lindner, Berichte Der Bunsengesellschaft Für Phys, Chemie 93 (1989) 535–536.
[70] S. Nath, P.K. Chattaraj, Pramana 45 (1995) 65–73.
[71] C.K. Ingold, Nature 145 (1940) 644–645.
[72] R.G. Parr, R.A. Donnelly, M. Levy, W.E. Palke, J. Chem. Phys. 68 (1978) 3801–3807.
[73] R.G. Pearson, Chemical Hardness: PEARSON:CHEM.HARDNESS O-BK, Wiley-VCH Verlag GmbH & Co. KGaA, Weinheim, FRG, 1997.
[74] R.G. Pearson, J. Am. Chem. Soc. 85 (1963) 3533–3539.
[75] R.G. Parr, R.G. Pearson, J. Am. Chem. Soc. 105 (1983) 7512–7516.
[76] R.G. Parr, L.v. Szentpály, S. Liu, J. Am. Chem. Soc. 121 (1999) 1922–1924.
[77] P.K. Chattaraj, U. Sarkar, D.R. Roy, Chem. Rev. 106 (2006) 2065–2091.
[78] W. Yang, W.J. Mortier, J. Am. Chem. Soc. 108 (1986) 5708–5711.
[79] R.G. Parr, W. Yang, J. Am. Chem. Soc. 106 (1984) 4049–4050.
[80] P.K. Chattaraj, S. Giri, S. Duley, Chem. Rev. 111 (2011) PR43–PR75.
[81] A. Morales-Bayuelo, J. Torres, R. Vivas-Reyes, Int. J. Quant. Chem. 112 (2012) 2637–2642.
[82] A. Morales-Bayuelo, H. Ayazo, R. Vivas-Reyes, Eur. J. Med. Chem. 45 (2010) 4509–4522.
[83] W. Brand-Williams, M.E. Cuvelier, C. Berset, LWT - Food Sci. Technol. 28 (1995) 25–30.
[84] Rikagu, CrystalClear Software Users Guide, version 1.3.6, 2009.
[85] G.M. Sheldrick, Acta Crystallogr. Sect. C Struct. Chem. 71 (2015) 3–8.
[86] O.V. Dolomanov, L.J. Bourhis, R.J. Gildea, J.A.K. Howard, H. Puschmann, J. Appl. Crystallogr. 42 (2009) 339–341.
[87] A.L. Spek, Acta Crystallogr. Sect. D Biol. Crystallogr. 65 (2009) 148–155.
[88] R.A. Friesner, J.L. Banks, R.B. Murphy, T.A. Halgren, J.J. Klicic, D.T. Mainz, M.P. Repasky, E.H. Knoll, M. Shelley, J.K. Perry, D.E. Shaw, P. Francis, P.S. Shenkin, J. Med. Chem. 47 (2004) 1739–1749.
[89] L. Ferreira, R. dos Santos, G. Oliva, A. Andricopulo, L.G. Ferreira, R.N. dos Santos, G. Oliva, A.D. Andricopulo, Molecules 20 (2015) 13384–13421.
[90] M.D. Eldridge, C.W. Murray, T.R. Auton, G.V. Paolini, R.P. Mee, J. Comput. Aided. Mol. Des. 11 (1997) 425–445.
[91] W.L. Jorgensen, D.S. Maxwell, J. Tirado-Rives, J. Am. Chem. Soc. 118 (1996) 11225–11236.